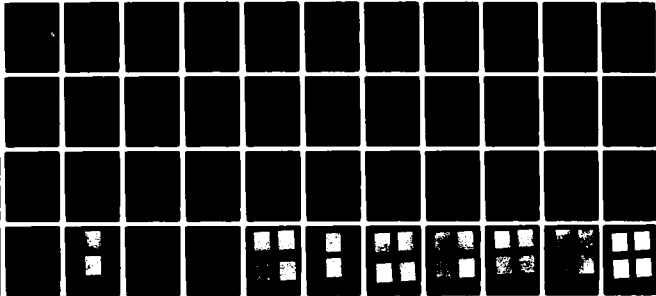AD-A112 758   DREXEL UNIV PHILADELPHIA PA DEPT OF MATERIALS ENGINEERING   F/G 11/6
                A FUNDAMENTAL STUDY OF TOOL STEELS PROCESSED FROM RAPIDLY SOLID--ETC(U)
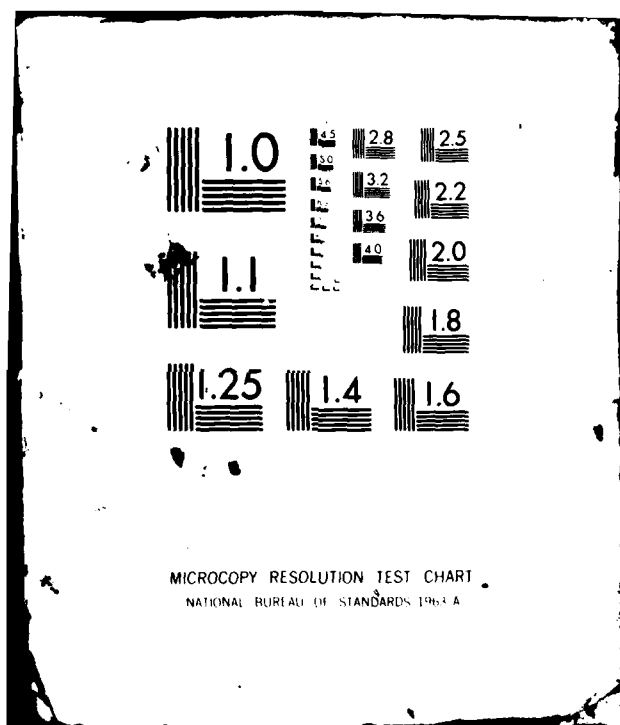   DEC 81   A LAWLEY, M J KOCZAK   N00014-81-K-0039
UNCLASSIFIED   NL

END
DATE
FILMED
4 82
DTIC

1.0

1.1

1.25 1.4 1.6

2.8 2.5
3.2 2.2
36
40 2.0

1.8

MICROCOPY RESOLUTION TEST CHART
NATIONAL BUREAU OF STANDARDS 1963 A

A FUNDAMENTAL STUDY OF TOOL STEELS

PROCESSED FROM RAPIDLY SOLIDIFIED POWDERS

A FUNDAMENTAL STUDY OF TOOL STEELS

PROCESSED FROM RAPIDLY SOLIDIFIED POWDERS

A. Lawley and M. J. Koczak

Annual Report - December 1981

(Contract #N00014-81-K0039)

for

Office of Naval Research

Metallurgy Branch

Arlington, Virginia 22217

Department of Materials Engineering
Drexel University
Philadelphia, Pennsylvania 19104

REPORT DOCUMENTATION PAGE		READ INSTRUCTIONS BEFORE COMPLETING FORM
1. REPORT NUMBER	2. GOVT ACCESSION NO. $AD.4112 75#$	3. RECIPIENT'S CATALOG NUMBER
4. TITLE *(and Subtitle)* A Fundamental Study of Tool Steels Processed From Rapidly Solidified Powders		5. TYPE OF REPORT & PERIOD COVERED Annual Report October 1980 – September 1981
		6. PERFORMING ORG. REPORT NUMBER
7. AUTHOR(s) A. Lawley and M. J. Koczak		8. CONTRACT OR GRANT NUMBER(s) N00014-81-K0039
9. PERFORMING ORGANIZATION NAME AND ADDRESS Drexel University Department of Materials Engineering Philadelphia, PA 19104		10. PROGRAM ELEMENT, PROJECT, TASK AREA & WORK UNIT NUMBERS
11. CONTROLLING OFFICE NAME AND ADDRESS Department of the Navy Materials Division Office of Naval Research Arlington, VA 22217		12. REPORT DATE December 1981
		13. NUMBER OF PAGES 49
14. MONITORING AGENCY NAME & ADDRESS *(if different from Controlling Office)*		15. SECURITY CLASS. *(of this report)* Unclassified
		15a. DECLASSIFICATION/DOWNGRADING SCHEDULE

16. DISTRIBUTION STATEMENT *(of this Report)*

DISTRIBUTION STATEMENT A

Approved for public release;
Distribution Unlimited

17. DISTRIBUTION STATEMENT *(of the abstract entered in Block 20, if different from Report)*

18. SUPPLEMENTARY NOTES

19. KEY WORDS *(Continue on reverse side if necessary and identify by block number)*

Atomization; tool steel powders; powder characterization, consolidation; heat-treatment; microstructure; properties.

20. ABSTRACT *(Continue on reverse side if necessary and identify by block number)*

The overall goal of this program is to establish quantitative processing-microstructure-property relationships in powder metallurgy tool steels. Powders of T15 and Rex 25 have been gas atomized and screened to specific particle size fractions to provide a spectrum of solidification rates, including the rapid solidification regime. Powders were then consolidated to full density by hot isostatic pressing. Atomized, annealed and consolidated powders of T15 have been characterized by means of optical and electron microscopy, x-ray

DD `FORM 1 JAN 73` 1473 EDITION OF 1 NOV 65 IS OBSOLETE

diffraction and hardness. To-date, a limited characterization of T15 after consolidation and heat-treatment has been accomplished. Similar studies have been initiated on the cobalt-free Rex 25 tool steel.

Cubic and hexagonal MC carbides in the form of interconnected networks are present in each size fraction of atomized powder. Carbide size decreases and particle hardness increases with decreasing particle size. The dependence of particle hardness on particle size is understood in terms of cooling rate, solid solution strengthening, the constituents and scale of the matrix and carbides, and the partitioning of alloying elements between matrix and carbides. After hot isostatic pressing, carbides are in the form of individual particles; three carbides have been identified namely cubic MC, cubic M_6C and cubic $M_{23}C_6$ in a matrix of α-ferrite. Carbide size increases as the isostatic pressing temperature increases and this results in a decrease in the hardness of the tool steel. For a given consolidation temperature, hardness is relatively independent of prior particle size fraction.

Properties and performance will be assessed in terms of bend strength, C-notch impact, wear , grindability, life and dimensional control during heat-treatment.
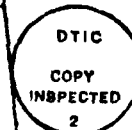
TABLE OF CONTENTS

SUMMARY

The overall goal of this program is to establish quantitiative processing-microstructure-property relationships in powder metallurgy tool steels. Powders of T15 and Rex 25 have been gas atomized and screened to specific particle size fractions to provide a spectrum of solidification rates, including the rapid solidification regime. Powders were then consolidated to full density by hot isostatic pressing. Atomized, annealed and consolidated powders of T15 have been characterized by means of optical and electron microscopy, x-ray diffraction and hardness. To-date, a limited characterization of T15 after consolidation and heat-treatment has been accomplished. Similar studies have been initiated on the cobalt-free Rex 25 tool steel.

Cubic and hexagonal MC carbides in the form of interconnected networks are present in each size fraction of atomized powder. Carbide size decreases and particle hardness increases with decreasing particle size. The dependence of particle hardness on particle size is understood in terms of cooling rate, solid solution strengthening, the constituents and scale of the matrix and carbides, and the partitioning of alloying elements between matrix and carbides. After hot isostatic pressing, carbides are in the form of individual particles; three carbides have been identified namely cubic MC, cubic M_6C and cubic $M_{23}C_6$ in a matrix of α-ferrite. Carbide size increases as the isostatic pressing temperature increases and this results in a decrease in the hardness of the tool steel. For a given consolidation temperature, hardness is relatively independent of prior particle size fraction.

Properties and performance will be assessed in terms of bend strength, C-notch impact, wear, grindability, life and dimensional control during heat-treatment.

I. INTRODUCTION

Over the past decade, significant progress has been made on new processes
for making fully-dense, high-performance materials by powder metallurgy (P/M).
In several cases, P/M processing is now a preferred alternative to conventional
ingot metallurgy (I/M) practice. Examples include hot isostatically pressed
(HIP), HIP and hot forged, or isothermally forged superalloy gas turbine discs,
extruded or hot forged high-strength aluminum alloys for aerospace structures,
HIP or HIP and hot-worked high speed tool steels and powder forgings of low
and medium alloy steels for load-bearing automotive components. Inherent
advantages in P/M processing include a high materials utilization factor,
fine scale microstructures, chemical homogeneity and alloying flexibility.
In the more highly alloyed compositions, it is frequently impossible to
process the material by conventional ingot metallurgy approaches involving
casting and working operations.

Successful development of high-performance P/M processing technology has
been vested primarily in improvements in powder making and consolidation.
Alloys are usually prepared by atomization since this approach offers a better
control on powder size, shape, chemistry and purity than chemical or electrolytic
methods of production. Commercial techniques are gas or water atomization,
soluble gas (vacuum) atomization and the rotating electrode process. Primary
consolidation techniques for these structural powder alloys include direct
compaction (e.g. hot isostatic pressing (HIP), the working of a powder
preform (e.g. powder forging, extrusion), or a combination of the above.

Integral to advances in atomization is the new technology of rapid solidi-
fication rate processing (RSR). RSR is a generic term that refers to
particulate production such that high cooling rates are achieved, typically
$> 10^4 °K/s$. Such cooling rates result in reduced microsegregation, elimination

-1-

of low incipient melt temperatures and ultra-fine microstructures. The implications of RSR processing are currently being examined in several alloy development programs for aluminum alloys, superalloys and specialty steels.

The goal of this basic research program is to establish detailed and quantitative processing - microstructure - property relationships in two P/M tool steels (T15 and Rex 25) in which particle cooling rate is a primary variable. A schematic of the overall program is given in Figure 1. Gas atomized powders of both T15 and Rex 25 have been made and screened to specific particle size fractions to provide a spectrum of powder particle solidification rates, including the rapid solidification regime. Screened powders were then consolidated to full density by hot isostatic pressing. To date, atomized, annealed and consolidated powders of T15 have been characterized by means of optical, scanning and transmission electron microscopy as well as by x-ray diffraction using diffractometer and Debye-Scherrer techniques. Microhardness measurements were also made on these powders. Hot isostatically pressed compacts have been similarly characterized. HIPed and heat-treated samples have been characterized to a limited extent in terms of their microstructure and hardness. Similar studies have recently been initiated on the Rex 25 P/M tool steel.

II. BACKGROUND

1. Powder Metallurgy (P/M) Tool Steels

Much of the work reported on high alloy P/M ferrous materials pertains to tool steels. Commercial practice involves gas atomization (nitrogen or oxygen) and consolidation by HIP (1,2). Compositions available include: M2S, M1, M3, M4, M7, M7S, M41, M42, M43S, T15 and M50.

These P/M tool steels exhibit a degree of alloy homogeneity and a fineness/uniformity of carbide dispersion that is significantly better than that achieved in the counterpart I/M tool steels and this gives rise to increased tool life (by a factor $\sim$2.5). Impact resistance and bend strength are also higher in the P/M processed tool steels. Other advantages of the P/M materials compared to I/M tool steels include shorter austenitizing times and a smaller out-of-roundness change during hardening.

Only a limited number of studies have been reported on the RSR processing of high alloy ferrous compositions. High-sulphur 303 stainless steel RSR powder exhibited significantly refined microstructures and microchemistries (1). These beneficial characteristics were retained during consolidation by hot extrusion. Fe-9Ni-4Co and Fe-2Mo consolidated from RSR powder exhibited a remarkable resistance to high-temperature grain coarsening (2). This was attributed to a fine-scale distribution of sulphides at prior powder particle boundaries.

Strutt (3) surface melted M2 tool steel by electron beam heating and achieved solidification rates $\sim$5 x 10^5°K/s. The prior melted zone contained δ - ferrite and fine-scale martensite which gave extremely high hardnesses (1100 VHN) on tempering compared to I/M material (850 VHN).

Rayment and Cantor (4) examined the as-quenched structure and hardness of a series of rapidly solidified iron-tungsten-carbon alloys ranging from

6 to 23 pct. tungsten with a constant W:C atomic ratio of 2:1. Similar studies were made on T1 high speed tool steels. Significant changes in microstructure and hardness were observed as the tungsten and carbon content increased. A change in structure from lath martensite to one consisting of δ-ferrite cells surrounded by austenite and M_6C carbide was observed with increasing tungsten content. After rapid solidification, the iron-tungsten-carbon alloys which were martensitic had a hardness of 700 kg/mm^2, whereas those containing δ-ferrite had a hardness between 1050 and 1100 kg/mm^2. It was observed that the as-quenched microstructure of the rapidly solidified steels was extremely sensitive to cooling rate. At cooling rates of 10^8 K/s, the structure was essentially all δ-ferrite. At cooling rates between 10^8 and 10^7 K/s, δ-ferrite cells were retained down to room temperature but were surrounded by regions of austenite and carbide (M_6C or M_2C). At lower cooling rates ($\leq 10^5$ K/s), little δ-ferrite was retained; the microstructure was austenitic with possibly some martensite. As the cooling rate reached that characteristic of bulk ingots (i.e. $<10^3$ K/s) the microstructure became predominantly martensitic. There was a small amount of retained austenite with a significant level of as-solidified carbides.

2. Ingot Metallurgy (I/M) Tool Steels

The microstructures and properties of conventionally processed high speed tool steels have been documented extensively. This information provides a base-line comparison for the current evaluation of P/M tool steels. Pertinent studies are summarized below.

Blickwede, Cohen and Roberts (5) examined a 6% tungsten, 5% molybdenum, 4% chromium high speed steel as a function of vanadium and carbon content, and as a function of heat-treatment temperature. Four non-matrix phases were found in the annealed and quenched conditions: M_6C - a complex

-4-

tungsten-molybdenum rich carbide; $M_{23}C_6$ - a chromium rich carbide; MC (or M_4C_3) - a vanadium rich carbide; M_3R_2 - essentially an iron-tungsten, molybdenum intermetallic compound. In the annealed condition, vanadium additions at any given carbon level promoted the formation of MC, causing the disappearance of $M_{23}C_6$ followed by M_6C. The compound M_3R_2 dissolved readily in the ferrite on heating, and since it carried no carbon with it to offset the influence of the ferrite-forming elements, the steels containing M_3R_2 could not be austenitized or quench-hardened. Among the carbides, $M_{23}C_6$ dissolved completely on heating, M_6C partially but MC hardly at all. The solution of $M_{23}C_6$ supplied sufficient carbon to austenitize the matrix and hence made it amenable to hardening.

Kayser and Cohen (6) examined several high-tungsten tool steels (T1, T2, T4, T15) and high-molybdenum tool steels (M10, M1, M2, M4). Each of the eight grades of high speed steel contained three carbide phases: M_6C - a tungsten-molybdenum-rich carbide, $M_{23}C_6$ - a chromium-rich carbide and MC - a vanadium-rich carbide. As a group, the tungsten grades contained larger percentages of carbides, both by weight and volume, than did the molybdenum-bearing grades. This was particularly true in the commercially hardened condition. The M_6C carbides usually predominated, but in the high carbon, high vanadium steels, the volume fraction of the MC carbides was equal to or higher than that of M_6C. In the annealed condition, all the steels contained ~10% $M_{23}C_6$ by volume; however, this carbide went into solution well below the usual hardening temperatures. M_6C and MC were partially dissolved during commercial austenitizing. Commercially hardened T15 was found to contain about 4% M_6C and 8% MC by volume, while T1 in a similar condition contained 0.3% MC and about 10% M_6C by volume. Except for chromium (and cobalt, if present), the bulk of the alloying elements in the annealed steels occurred in the carbide phases.

Goldschmidt (7) carried out elaborate x-ray investigations on filings and carbides extracted from high-speed 18-4-1 type steels. Apart from the austenite-to-martensite transformation, a variety of changes in carbide structure occurred on hardening and tempering and with varying alloying content. The η carbide (M_6C (Fe_4W_2C/Fe_3W_3C)) was always predominant and frequently was the only carbide present; however, additional compounds formed were: (a) the κ carbide ($M_{23}C_6$ = (Cr, Fe, W, Mo)$_{23}C_6$); (b) an iron-tungsten intermetallic compound ξ'; (c) a transitory precipitate between η and κ, revealed only after restricted tempering conditions; (d) a carbide V_4C_3 with a rock salt structure, which occurred only if the steel was vanadium rich, lesser amounts of vanadium (and of chromium) entering η and κ. Internal changes in lattice parameter occurred within the η carbide. A new η-carbide (η*) of greatly contracted cube edge was observed, which was formed with the simultaneous liberation of tungsten. The partitioning of alloying elements between the matrix and carbides varied with heat treatment; cobalt, for example, was observed initially (i.e., after hardening and light tempering) to reside entirely in the austenite and martensite, but on prolonged tempering it migrated partially into the carbide.

Similar work by Malkiewicz et al. (8) on two grades of high speed steel, 18-4-1 and 9-4-2, showed that the predominant carbide in both types of steel was M_6C which differed in chemical composition according to the type of steel. The presence of $M_{23}C_6$, M_7C_3 and MC carbides was established. $M_{23}C_6$ and M_7C_3, both chromium-rich carbides, dissolved during austenitizing up to 1100°C. Extensive solution of tungsten and vanadium in the matrix began at about 1200°C.

Thus, excess carbides exert a direct influence on the properties of high speed steel: In addition, they govern the composition of the matrix through

the degree of solution effected by the austenitizing treatment. Consequently, the hardening and tempering characteristics of the steel are influenced by the structure, stoichiometry, solubility and stability of the carbides.

III. PROCEDURE

1. Powder Production

Heats of T15 and Rex 25 high speed tool steels have been atomized at the Materials Research Center, Crucible Inc. The alloy charge was melted in a nitrogen atmosphere and nitrogen gas atomized. Powder was collected in liquid nitrogen at the base of the atomizing unit.

Chemical analyses of the two batches of powder are summarized in Table I. Typical compositions for corresponding commercial alloy powders and the ingot metallurgy counterpart are included in Table I for purposes of comparison. The levels of the alloying elements in the powders atomized for this research program are similar to those in the commercial Crucible Particulate Metallurgy T15 and Rex 25 tool steels. The four powder size fractions selected for study are listed in Table II.

2. Powder Characterization

Initially, T15 powders corresponding to the four different size fractions listed in Table III were characterized both in the as-atomized condition and after annealing at 1125°C (2060°F) for 30 minutes. These size fractions are not identical to those used subsequently in the major part of the study; however, they provide a broader size range survey than those listed in Table II. Powder annealing at 1125°C (2060°F) was carried out in a regular box furnace. Atmosphere control was achieved by wrapping the tool steel powders in Sen/Pak heat treating containers. Powders in the atomized as well as in the annealed condition were characterized in terms of their microstructure, microhardness and the phases present.

a. Atomized Powders

Each of the two powders (T15 and Rex 25) in the four size ranges listed in Table III was examined by SEM in order to obtain an initial

appreciation for overall powder shape and surface condition.

Optical microscopy on mounted, polished and etched powders proved unsatisfactory due to an inability to resolve the extremely fine scale structure inherent in the four size fractions of powder particles. To achieve higher resolution, conventional two-step replicas were prepared from the polished and etched powder particle surfaces. These replicas were examined by TEM in a JEM 120 microscope.

Microhardness measurements were made on the atomized powders using standard techniques.

X-ray diffraction (Debye-Scherrer method) was used to evaluate the phases present in the atomized powders using chromium radiation. The use of a vanadium oxide filter significantly reduced the intensity of the κ_β radiation. The presence of iron in the sample resulted in the choice of chromium as the target material; this minimized fogging of the film. However, the presence of tungsten (L lines of tungsten) also posed a problem in terms of a high level of fogging of the film. Finally, the strain induced in the structure due to the high cooling rates caused an increase in the level of background radiation. The diffraction patterns thus obtained were used primarily to evaluate the matrix phase.

Subsequently, powders corresponding to each of the four size fractions were treated with an 8% bromine methanol solution in order to dissolve away the matrix. The residue, consisting of the excess phases, was examined by x-ray diffraction, as described above.

b. Annealed Powders

Powders were annealed at 1125°C (2060°F) for 30 minutes. Samples from each of the four size fractions (Table III) were then characterized by electron microscopy (TEM of replicas) and x-ray diffraction.

3. Powder Consolidation

Small bar samples (1" x 6" (25.4 mm x 152.4 mm)) of each alloy in each of the four powder size ranges (Table II) were hot outgassed, sealed and hot-isostatically pressed at 1195°C (2185°F) or 1130°C (2065°F). The former is the standard temperature used by Crucible Inc. for commercial P/M high-speed tools teels. The lower temperature was used as a possible means for grain size control during densification in the HIP cycle. This yielded a matrix of eight samples for each composition, i.e. four size fractions and two HIP temperatures.

The purpose of the small samples was to verify that HIP consolidation had brought about complete densification. Subsequently, larger compacts [4"(101.6 mm) diameter x 11"(279.4 mm) length] will be produced by HIPing of the bulk of the powder. Each of the small bar samples has been cut in half for purposes of microstructural characterization and preliminary examination of heat-treatment response. The system of coding used is given in Table IV.

4. Characterization of the HIPed Material

Each of the eight T15 samples was mounted, polished and etched using Kalling's Reagent. Two-stage carbon replicas of the samples were prepared and examined by TEM. Rockwell hardness measurements were carried out on each of the eight samples.

X-ray diffraction patterns were obtained using diffractometry and the Debye-Scherer technique. The former was used essentially to evaluate the matrix phase. The Debye-Scherrer method was used to identify the excess phases. To this end, isolation of the carbides from the consolidated material was achieved by electrolytic extraction. Details of the extraction technique have been documented elsewhere (9). This procedure was followed for each of the eight T15 compacts.

5. Heat Treatment of the Consolidated Material

A study of the heat treatment response of material cut from the small HIP bars (T15) has been initiated. Two austenitizing temperatures, 1176°C (2150°F) and 1226°C (2240°F), were selected. Samples were preheated at 815°C (1500°F). The samples were heated to the austenitizing temperature and held at temperature for four minutes before oil quenching. Three tempering temperatures were selected (538°C (1000°F), 552°C (1025°F) and 565°C (1050°F)). A coding system for the various processing treatments is given in Table IV.

6. Characterization of the Heat-Treated Material

The heat treatment schedule yielded a matrix of forty-eight samples (8 HIPed samples x 2 austenitizing temperatures x 3 tempering temperatures) per composition, each of which had been subjected to a specific heat treating sequence. To date, selected samples from this matrix have been characterized in terms of microstructures and hardness. Further microstructural characterization will be made using TEM and x-ray diffraction. A similar study will then be carried out on the Rex 25 P/M tool steel.

IV. RESULTS

1. Atomized Powders

To obtain an initial appreciation for overall powder shape and
surface condition, atomized powder (T15) in the four size ranges (Table III)
was examined by SEM. Representative SEM micrographs are shown in Figures 2(a),
2(b) and 2(c). Particles are generally spherical in shape with relatively
smooth surfaces. At each size fraction, small satellites are present
attached to the main powder particles.

Representative TEM micrographs of two step replicas prepared from three
size fractions of atomized powder are compared in Figures 3(a), 3(b) and 3(c).
It is seen that the carbides (major phase) are in the form of an interconnected
network, rather than as discrete particles. The size of these carbides decreases
with decreasing particle size.

Identification of the matrix by x-ray diffraction is not yet complete.
The presence of a high level of background radiation, line broadening due to
lattice strains and overlapping of lines corresponding to matrix phase(s) and
excess phases have hindered unambiguous identification. Efforts are now being
made to prepare thin foils for TEM in the conventional diffraction contrast
mode.

Debye-Scherrer diffraction patterns of the excess phase residue from each
of the four size fractions are consistent with MC-type carbides. Two types of
MC carbide were identified, namely a cubic and a hexagonal form. Lattice
parameters were determined in each case, Table V; the lattice parameters are
plotted as a function of particle size in Figure 4.

Microhardness data for the atomized powder are presented in Figure 5.
Hardness increases with decreasing particle size.

-12-

2. Annealed Powders

Representative TEM micrographs of two step replicas prepared from annealed powder corresponding to the coarsest and finest-size fractions are illustrated in Figures 6(a) and 6(b) respectively. These micrographs show that after annealing, the carbides exist as individual particles. The carbides are finer in the -400 mesh powder than in the -10+20 size fraction.

X-ray diffraction analysis of the annealed powder shows that in each size fraction the matrix is α-ferrite. The variation of the lattice parameter of the α-ferrite matrix with particle size is given in Figure 7.

X-ray diffraction analysis of material extracted from the matrix shows that the phases present are cubic MC and cubic M_6C-type carbides. These were found to be a common feature in each of the four size fractions evaluated. The variation of carbide lattice parameters with powder particle size is plotted in Figure 7. In addition, it was observed that the diffraction pattern from the coarsest size fraction showed a trace of hexagonal γ-MC. The phases present in the annealed powder and the corresponding lattice parameter values are summarized in Table VI.

For a given powder size fraction, the particle hardness is lowered by annealing. The decrease is larger for the -400 mesh fraction compared to the -10+20 fraction. From Figure 8 it is seen that the lowest hardness values occur at the intermediate size fractions.

3. Consolidated Material

TEM micrographs of two-step replicas of the consolidated samples corresponding to the coarsest and finest size fractions are shown in Figures 9(a), 9(b), 10(a) and 10(b). Figures 11(a) and 11(b) are TEM micrographs of HIPed samples obtained from a -20 mesh blend. In all cases, it is seen that the carbides are coarser following the higher consolidation temperature. Also, for a particular consolidation temperature, the carbides are approximately the

same size in the coarsest and finest size fractions. Figure 9(b),which is a micrograph of a sample corresponding to the coarsest size fraction HIPed at the higher of the two temperatures, shows three different types of carbides: (i) a blocky (massive) type, (ii) a small globular type, and (iii) strands or ribbons. These features are also evident in Figures 10(b) and 11(b) which represent the finest size fraction and the commercial blend (-20 mesh) respectively. Both powders were HIPed at the higher temperature. In the case of powder consolidated at the lower temperature, these features are present but are not as pronounced (Figures 9(a), 10(a) and 11(a)).

From x-ray diffraction analysis, it was found that in all cases the matrix of the HIPed material was α-ferrite. Lattice parameter data for the α-ferrite are given in Table VII. In each of the eight conditions (two HIP temperatures and four size fractions) Debye-Scherrer analysis of the material extracted from the matrix confirmed the presence of three phases: cubic MC carbide (usually vanadium-rich); cubic M_6C carbide (usually iron-tungsten rich) and cubic $M_{23}C_6$ (usually chromium-rich). Lattice parameters were determined and values are listed in Table VIII.

Hardness measurements on the consolidated samples show that for each consolidation temperature, hardness variation with particle size fraction is minimal. However, the hardness of the samples HIPed at the lower temperature is on the average higher than that for samples HIPed at the higher temperature (Table IX).

4. Consolidated and Heat-Treated Material

To date a limited number of heat-treated samples have been examined. Figures 12(a) and 12(b) are optical micrographs of oil-quenched samples; both correspond to the finest size fraction and the lower of the two HIPing temperature. The austenitizing temperatures were 1176°C (2150°F) and 1226°C (2240°F), respectively. Prior austenite grain boundaries are evident and it

-14-

is clear that the austenitizing temperature has a strong influence on grain
size. Carbides are present within the grains and at grain boundaries. In
comparison, corresponding optical micrographs for the coarsest size fraction
and the lower of the two HIPing temperatures are shown in Figures 13(a) and
13(b). Again, the grain size is much larger following austenitization at
the higher temperature. However, comparing Figures 12(a) and 13(a) and
Figures 12(b) and 13(b), it is evident that grain size is relatively insensitive
to the prior particle size fraction.

Representative TEM micrographs of the HIPed and heat treated material
consolidated from the (-20+60) size fraction are compared in Figures 14(a),
14(b), 14(c) and 14(d). These micrographs pertain to the lower HIPing
temperature (1130°C (2065°F)) and lower austenitizing temperature (1176°C (2150°F)).
It is seen that carbide size increases with increasing tempering temperature.
The appearance of the matrix is different in Figure 14(a) than in Figures 14(b),
14(c) and 14(d). Figures 15(a), 15(b), 15(c) and 15(d) are microstructures of
material HIPed at the same temperature (1130°C (2065°F)) except that the austeni-
tizing temperature was 1226°C (2240°F). Again, it is seen that there is a gradual
increase in carbide size with increasing tempering temperature. Comparison of
Figure 14(a) with Figure 15(a) or Figure 14(d) with Figure 15(d) shows that the
difference in carbide size as a consequence of the higher austenitizing
temperature is minimal.

TEM micrographs of HIPed and heat-treated material corresponding to the
-325 mesh size fraction are shown in Figures 16(a), 16(b), 16(c) and 16(d) and
Figures 17(a), 17(b), 17(c) and 17(d). These samples were all hot isostatically
pressed at 1130°C (2065°F) and subsequently heat-treated. Here, too, all of
the above observations are repeated. A comparison of Figure 14(a) with Figure
16(a) and Figure 15(a) with Figure 17(a) shows that the prior particle size
has little influence on carbide size. Similar conclusions are drawn from a

-15-

comparison of Figure 14(c) and Figure 15(c) with Figure 16(c) and Figure 17(c), respectively.

Hardness measurements of the heat-treated samples are given in Table X. For compacts pressed at 1130°C (2065°F) from the -20+60 size fraction and subsequently heat-treated, the austenitizing temperature influences the hardness response of the tempered material. It can be seen, in Figure 18, that for samples austenitized at 1176°C (2150°F), the quenched hardness is higher than the quenched and tempered hardness; also hardness decreases with increasing tempering temperature. However, for the material austenitized at 1226°C (2240°F), the as-quenched hardness is lower than the value obtained after tempering at 538°C (1000°F), Figure 18. Here, too, the hardness decreases with increasing tempering temperature.

Similar measurements were made on the heat-treated material from the finest size fraction. In this case, for samples austenitized at 1176°C (2150°F) and 1226°C (2240°F), the hardness response was similar. Here, the as-quenched hardness is higher than the quenched and tempered value; however, hardness increases and then decreases with increasing tempering temperature (Table X, Figure 18).

V. DISCUSSION

1. Atomized Powders

The microhardness of the powders in the atomized condition increases with decreasing particle size, Figure 5. This behavior can be attributed to the following factors: (i) cooling rate, (ii) solid solution strengthening, (iii) size and nature of the matrix and carbide phases. Figures 3(a), 3(b) and 3(c) show that with a decrease in particle size, there is a decrease in the size and amount of carbides. In the case of the -400 mesh size fraction, carbides are not resolved, at magnifications up to 7000X. This would imply that the major portion of the alloying elements is in solid solution in the matrix. The finer the size of the particle, the higher is the cooling rate. With increase in cooling rate, increasing amounts of δ-ferrite can be retained in the matrix. This increases the matrix hardness because δ-ferrite is known to be harder than martensite[4]. This also results in increased hardness. Finally, the finer nature of the carbides, and possibly a finer matrix grain size, can cause an increase in hardness.

Figure 4 is a plot of lattice parameter as a function of particle size for the excess phases MC and γ-MC. Both of these carbides are vanadium-rich. MC carbide has an fcc structure, while γ-MC has a hexagonal structure. The prototype of the MC carbide is V_4C_3 while that for γ-MC is VC. Also given in Figure 4 are the c/a values for each size fraction. Table XI gives the atomic radius of all the major elements present in T15 tool steels.

The lattice parameter for cubic MC carbide increases with increasing particle size, Figure 4. The a_0 value for the -400 mesh powder is very close to the a_0 value of pure vanadium carbide (V_4C_3). This implies that the MC carbides in this size fraction must be vanadium-rich with a small percentage of the alloying elements replacing vanadium. This is expected because vanadium

-17-

is the strongest carbide-former of all the alloying elements present in the powders. At the extremely high cooling rates required to produce this fine size fraction (-400 mesh), diffusion is limited, therefore the matrix is supersaturated. These arguments also hold true in the case of the hexagonal γ-MC carbide. Figure 4 shows that the c_0 value for the -400 mesh powders is slightly higher than that for pure γ-VC. This would imply limited diffusion of W into the lattice replacing vanadium, Table XI. With an increase in particle size (and an associated decrease in cooling rate), it is seen that the lattice parameter increases. This is due to the partitioning of the elements present. The extent of partitioning is yet to be determined accurately. However, the increase in lattice parameter suggests that more and more tungsten (next to vanadium in strength as a carbide-former) enters the MC and γ-MC type carbides. This is due to the slower and slower cooling rates with increasing particle size. This behavior also ties in with Figure 5 which is a plot of microhardness as a function of particle size. As more and more of the tungsten comes out of the matrix, the microhardness decreases. This is due to the difference in the atomic radii of tungsten and iron which causes lattice strain in the matrix, Table XI. Of interest is the fact that the c_0/a_0 ratio remains essentially constant for all size fractions.

2. Annealed Powders

For the annealed powders, microhardness as a function of particle size is shown in Figure 8. It is seen that microhardness decreases, then increases with increasing particle size. This behavior is possibly due to the fact that for the coarsest size fraction, the powder was not fully annealed. This statement can be further substantiated by the fact that traces of meta-stable γ-MC were detected in the -10+20 size fraction. Comparing Figures 8 and 5, it is seen that in all cases the microhardness decreases on annealing. This

behavior is due to the combined effect of the following features: (i) reduction in lattice strain, (ii) change in the size and shape of the excess phases, Figures 6(a) and 6(b), (iii) dissolution of the hard hexagonal metastable γ-MC, (iv) more alloying elements entering the excess phases, (v) change of the matrix from martensite or δ-ferrite to α-ferrite, and (vi) more carbon moving out of the matrix in order to form new stable carbides. However, although the hardness values are lower in comparison to the atomized powders, on an absolute scale, they are still high. This is due to the precipitation of new carbides on a fine scale. A comparison of Figures 5 and 8 also shows that the change in microhardness before and after annealing is higher in the coarser size fractions. This is possibly due to the coarser carbides in the case of the higher size fractions.

Lattice parameters of α-ferrite, MC carbide and M_6C carbides as a function of particle size in the annealed powders have been plotted in Figure 7. M_6C is an Fe_3W_3C - Fe_4W_2C type carbide. The average lattice parameter of Fe_3W_3C - Fe_4W_2C is 11.04 Å. The -400 mesh powder has a_{M_6C} = 11.056 Å. This is a small increase over the 'a' value for Fe_3W_3C - Fe_4W_2C. This would imply that the iron in M_6C is partially replaced by an element of larger atomic radius such as chromium or vanadium. On annealing the -400 mesh powder, γ-MC goes into solution, and M_6C precipitates. γ-MC (400 mesh) had mostly vanadium but some tungsten in it. Thus, most of the vanadium which comes out of γ-MC as well as most of the tungsten in the matrix (in the atomized condition) precipitate out as M_6C. The appreciable increase in a_{MC} in the annealed condition over a_{MC} in the atomized condition implies that some of the tungsten has gone into the MC carbides. Some of the iron in the matrix goes into M_6C, and chromium takes its place causing the small increase in the lattice parameter of α-ferrite over that of pure α-iron. This increase can also be partially due to the carbon present in the matrix.

-19-

For the -200+230 size fraction, the MC carbides exhibit the same lattice parameter before and after annealing, cf. Figures 4 and 7. The γ-MC in the atomized condition for this size fraction is richer in tungsten than for the -400 mesh size. This means on dissolution of γ-MC, more tungsten and less vanadium enters the matrix compared to the -400 mesh size fraction. However, the amount of carbon available is fixed. Some of the tungsten stays in the matrix causing an appreciable increase in the lattice parameter of the matrix over the -400 mesh. The reason for this is probably the stronger tendency of vanadium over tungsten to form carbides.

For the -40+45 mesh size, the situation is similar except that there is an appreciable increase in the lattice parameter of M_6C. This is possibly due to the iron in M_6C being displaced by more chromium and vanadium from the matrix and simultaneously resulting in a small decrease in the lattice parameter of the matrix. In addition, the decrease in the lattice parameter of MC (annealed) over MC (atomized) causes the liberation of some tungsten which goes into the matrix and offsets the effect of chromium and vanadium leaving the matrix.

In the case of the -10+20 size fraction, the presence of traces of γ-MC depletes the matrix of W and V to a greater extent than in the other size fractions, resulting in a decrease in a_o of the matrix. A decrease in the availability of tungsten also causes an increase of chromium and vanadium in M_6C, causing a decrease in the lattice parameter. This effect is evidenced to a lesser extent in MC carbides.

These explanations must be considered somewhat speculative at this time due to insufficient quantitative data. The main objective has been to attempt an explanation consistent with all the observed data.

3. Consolidated Material

For a particular HIPing temperature, the hardness is approximately the same for the different size fractions, as well as for a commercial blend. However, it is lower for a higher HIPing temperature, Table IX. This is due to the coarsening of the excess phases, Figures 9(a), 9(b), 10(a), 10(b), 11(a) and 11(b).

For both HIPing temperatures, the phases present are α-ferrite and MC, M_6C and $M_{23}C_6$ carbides. In the case of α-ferrite, the lattice parameters are approximately the same for all size fractions, Table VII. Lattice parameters for the MC, M_6C and $M_{23}C_6$ also behave in a similar manner, Table VIII. The small variations in the lattice parameter values could possibly be due to experimental error.

4. Heat Treated Material

Hardness measurements on the heat treated samples have been plotted as a function of the tempering temperature as well as the austenitizing temperature in Figure 18. For either size fraction, hardness in the as-quenched condition is higher for the lower of the two austenitizing temperatures. Two features contribute to this behavior: (i) the finer grain size obtained by austenitizing at a lower temperature, (ii) a lesser amount of the hard excess phases going into solution at the lower austenitizing temperature. However, a third feature, namely the extent of solid solution strengthening is lower at the lower austenitizing temperature. For a particular tempering temperature, the hardness is higher for the sample austenitized at the higher of the two temperatures 1226°C (2240°F); 1176°C (2150°F). This behavior is attributed to the precipitation of new carbides. When samples are austenitized at the higher of the two temperatures, there is a greater degree of carbide-dissolution. On quenching, these samples exhibit a greater

deviation from equilibrium in terms of carbon supersaturation. Therefore, when tempered, they precipitate carbides more readily than do samples austenitized at the lower temperature.

For the -325 mesh size, hardness decreases, then increases and again decreases on tempering. The secondary hardening peak is possibly associated with the precipitation of new carbides; Figure 18. With increasing tempering temperature, the precipitates coarsen, and the hardness decreases. The coarsest size fraction, austenitized at 1176°C (2150°F), exhibits a continuous decrease in hardness with increasing tempering temperature. In comparison, a similar sample austenitized at 1226°C (2240°F) exhibits an initial increase in hardness before decreasing with increasing tempering temperature. This behavior can be attributed to the increased degree of carbide dissolution at the higher temperature and therefore a greater level of supersaturation in the quenched structure. Therefore, on tempering, carbide precipitation is enhanced, resulting in an increase in hardness.

VI. FUTURE WORK

Future work on powders will icnlude TEM (diffraction contrast) and STEM (microchemistries). STEM will also be employed to examine composition profiles in carbides estracted from HIPed and HIPed and heat-treated material. Further x-ray studies, hardness determinations and TEM of replicas will be carried out on HIPed and heat-treated material.

Larger compacts have been HIPed and will be forged to selected deformation levels. Studies as described above will then be made on the consolidated and forged material in order to assess the effects of deformation processing on structure.

In the second year of this research program, a property evaluation will be initiated. This will include:

  (i)   Bend strength

  (ii) C-notch impact

 (iii) Wear

  (iv) Grindability

  (v)   Life

  (vi) Dimensional stability

Work on the Rex 25 P/M tool steel, initiated part way through the first year will be continued. The approach will be similar to that described above and will provide for a comparison with T15 in terms of the role of cobalt.

REFERENCES

1. Kelly, T.F. and Vander Sande, J.B., "A STEM Analysis of Two Rapidly
   Solidified Stainless Steels", <u>Rapid Solidification Processing - Principles
   and Technologies II</u>; Editors: R. Mehrabian, B. H. Kear and M. Cohen,
   Claitors Publishing Division, p. 100, 1980.

2. Suga, M., Goss, J.L., Olson, G.B. and Vander Sande, J.B., "Austenitic
   Grain Growth Characteristics in Rapidly Solidified Martensitic Steels",
   ibid. ref. 1.

3. Strutt, P.R., Kurup, M. and Gilbert, D.A., "Comparative Study of Electron
   Beam and Laser Melting of M2 Tool Steel", ibid. ref. 1.

4. Rayment, J.J. and Cantor, B., "The As-Quenched Microstructure and Tempering
   Behavior of Rapidly Solidified Tungsten Steels", Met. Trans. A, p. 1557,
   Vol. 12A, 9, 1981.

5. Blickwede, D.J., Cohen, M. and Roberts, G.A., "The Effect of Vanadium and
   Carbon on the Constitution of High Speed Steels", ASM Trans., p. 1161,
   Vol. 42, 1950.

6. Kayser, F. and Cohen, M., "Carbides in High Speed Steel - Their Nature and
   Quantity", Metal Progress, p. 79, Vol. 61, 6, 1952.

7. Goldschmidt, H.J., "Structure of Carbides in Alloy Steels - Part II:
   Carbide Formation in High-Speed Steels", Journal of the Iron and Steel
   Institute, p. 189, Vol. 170, 1952.

8. Malkiewicz, T., Bojarski, Z. and Foryst, J., "Carbides in Annealed and
   Quenched High-Speed Steels", Journal of the Iron and Steel Institute,
   p. 25, Vol. 193, 1959.

9. Blickwede, D.J. and Cohen, M., "The Isolation of Carbides from High Speed
   Steel", Trans. of American Inst. of Mining, Metallurgical and Petroleum
   Engineers, p. 578, Vol. 185, 1949.

Table I: Chemical Analyses of Powder and Ingot Metallurgy
High Speed Tool Steels (Weight%)

Alloy	Alloy Form	C	Cr	Co	W	V	Mo	Mn	Si	O_2	N_2
TI5	Powder/This Program	1.52	4.67	5.22	12.19	4.85	---	0.31	0.46	0.0063	0.1
Rex 25	Powder/This Program	1.79	3.01	---	13.29	4.63	6.52	0.31	0.46	0.0061	0.1
TI5	Powder/Commercial	1.48	4.00	4.59	12.12	4.65	0.58	0.32	0.42	0.008	0.057
Rex 25	Powder/Commercial	1.81	4.04	0.48	12.46	4.95	6.48	0.40	0.33	0.013	0.086
TI5	Ingot/Commercial	1.57	4.62	5.10	13.59	4.86	0.69	0.30	0.21	---	---
Rex 25	Ingot/Commercial	1.82	4.11	0.28	12.35	5.18	6.48	0.34	0.39	---	0.039

Table II: Powder Size Fractions and Cooling Rates

U.S. Standard Sieve #	Size (μm)	Approximate Minimum Cooling Rate (°K/S)
-20	≤ 840	5×10^3
-20 +60	250 - 840	2×10^4
-150 +325	44 - 100	10^5
-325	≤ 44	$> 10^5$

Table III: Size Fractions for Preliminary Powder Characterization Studies

U.S. Standard Sieve #	Size (μm)
-10 +20	840 - 2000
-40 +45	350 - 420
-200 +230	62 - 74
-400	≤ 37

Table IV: Coding System for Powder Consolidation and Heat Treatment

Code	Interpretation
H1	Hot Isostatically Pressed at 1130°C (2065°F)
H2	Hot Isostatically Pressed at 1195°C (2185°F)
A1	Austenitized at 1176°C (2150°F) for 4 mins. and oil-quenched
A2	Austenitized at 1226°C (2240°F) for 4 mins. and oil-quenched
T1	Tempered for (2 + 2 + 2) hrs. at 538°C (1000°F)
T2	Tempered for (2 + 2 + 2) hrs. at 552°C (1025°F)
T3	Tempered for (2 + 2 + 2) hrs. at 565°C (1050°F)

Table V: **Atomized Powder (T15)-Lattice Parameters of Excess Phases**

Size Fraction	Excess Phases Present	Lattice Parameter (Å)		
$-10 + 20$	Cubic MC	a_o	=	4.183 Å
	Hexagonal γ – MC	a_o	=	2.91 Å
		c_o	=	4.645 Å
		c_o/a_o	=	1.596 Å
$-40 + 45$	Cubic MC	a_o	=	4.182 Å
	Hexagonal γ – MC	a_o	=	2.912 Å
		c_o	=	4.625 Å
		c_o/a_o	=	1.590 Å
$-200 + 230$	Cubic MC	a_o	=	4.173 Å
	Hexagonal γ – MC	a_o	=	2.88 Å
		c_o	=	4.63 Å
		c_o/a_o	=	1.607 Å
-400	Cubic MC	a_o	=	4.160 Å
	Hexagonal γ – MC	a_o	=	2.883 Å
		c_o	=	4.595 Å
		c_o/a_o	=	1.60 Å

Table VI: <u>Annealed Powder (T15)*– Lattice Parameters of Matrix and Excess Phases</u>

Size Fraction	Phases Present		Lattice Parameter (Å)
-10 + 20	Matrix : α – ferrite		a_o = 2.877 Å
	Carbides: Cubic MC		a_o = 4.182 Å
		Cubic M_6C	a_o = 11.082 Å
		Hexagonal MC (traces)	
-40 + 45	Matrix : α – ferrite		a_o = 2.885 Å
	Carbides: Cubic MC		a_o = 4.179 Å
		Cubic M_6C	a_o = 11.090 Å
-200 + 230	Matrix : α – ferrite		a_o = 2.886 Å
	Carbides: Cubic MC		a_o = 4.178 Å
		Cubic M_6C	a_o = 11.062 Å
-400	Matrix : α – ferrite		a_o = 2.869 Å
	Carbides: Cubic MC		a_o = 4.177 Å
		Cubic M_6C	a_o = 11.056 Å

* 1125°C (2060°F) for 30 minutes.

Table VII: <u>HIPed Material - Lattice Parameter of Matrix Phase</u>

Sample	Matrix Phase	Lattice Parameter (Å)
−20 + H1	α − ferrite	a_o = 2.870 Å
−20 + H2	α − ferrite	a_o = 2.872 Å
(−20 + 60)+ H1	α − ferrite	a_o = 2.872 Å
(−20 + 60)+ H2	α − ferrite	a_o = 2.872 Å
(−150 + 325)+ H1	α − ferrite	a_o = 2.871 Å
(−150 + 325)+ H2	α − ferrite	a_o = 2.870 Å
−325 + H1	α − ferrite	a_{oo} = 2.870 Å
−325 + H2	α − ferrite	a_o = 2.871 Å

Table VIII: __HIPed Material – Lattice Parameter of Excess Phases__

Sample	Excess Phases	Lattice Parameter (Å)
−20 + H1	Cubic MC Cubic M_6C Cubic $M_{23}C_6$	a_o : 4.183 Å a_o : 11.059 Å a_o : 10.581 Å
−20 + H2	Cubic MC Cubic M_6C Cubic $M_{23}C_6$	a_o : 4.182 Å a_o : 11.058 Å a_o : 10.586 Å
(−20 + 60)+ H1	Cubic MC Cubic M_6C Cubic $M_{23}C_6$	a_o : 4.179 Å a_o : 11.059 Å a_o : 10.604 Å
(−20 + 60)+ H2	Cubic MC Cubic M_6C Cubic $M_{23}C_6$	a_o : 4.187 Å a_o : 11.071 Å a_o : 10.606 Å
(−150 + 325)+ H1	Cubic MC Cubic M_6C Cubic $M_{23}C_6$	a_o : 4.176 Å a_o : 11.053 Å a_o : 10.567 Å
(−150 + 325)+ H2	Cubic MC Cubic M_6C Cubic $M_{23}C_6$	a_o : 4.184 Å a_o : 11.057 Å a_o : 10.588 Å
−325 + H1	Cubic MC Cubic M_6C Cubic $M_{23}C_6$	a_o : 4.178 Å a_o : 11.054 Å a_o : 10.582 Å
−325 + H2	Cubic MC Cubic M_6C Cubic $M_{23}C_6$	a_o : 4.182 Å a_o : 11.056 Å a_o : 10.592 Å

Table IX: Hardness of HIPed Material

Sample	R_c*	Sample	R_c*
−20 + H1	35.0	−20 + H2	30.0
(−20 + 60)+ H1	36.2	(−20 + 60)+ H2	31.5
(−150 + 325)+ H1	33.0	(−150 + 325)+ H2	30.0
−325 + H1	33.0	−325 + H2	29.0

* Average of 5 readings

Table X: Hardness of HIPed and Heat Treated Material

Sample	R_c*	Sample	R_c*
(−20 + 60)+ H1 + A1	65.5	(−20 + 60)+ H1 + A2	64.2
(−20 + 60)+ H1 + A1 + T1	64.4	(−20 + 60)+ H1 + A2 + T1	66.3
(−20 + 60)+ H1 + A1 + T2	63.3	(−20 + 60)+ H1 + A2 + T2	64.7
(−20 + 60)+ H1 + A1 + T3	61.5	(−20 + 60)+ H1 + A2 + T3	63.3
Sample	R_c*	Sample	R_c*
−325 + H1 + A1	66.2	−325 + H1 + A2	65.9
−325 + H1 + A1 + T1	64.0	−325 + H1 + A2 + T1	65.5
−325 + H1 + A1 + T2	64.7	−325 + H1 + A2 + T2	65.5
−325 + H1 + A1 + T3	62.4	−325 + H1 + A2 + T3	63.7

* Average of 5 readings

Table XI: <u>Atomic Radius of Iron and Some Alloying Elements</u>

Element	Atomic Radius (Å)
C	0.914
Co	1.25
Fe	1..26
Cr	1.30
V	1.34
W	1.41

```
                    ┌─────────────────────┐
                    │ Atomize 500 pounds of│
                    │   T15 and Rex 25    │
                    └─────────────────────┘
                              │
                    ┌─────────────────────┐
                    │ Screen powder to four│
                    │ (4) different particle│
                    │   size fractions.   │
                    │ Yield ~200 pounds/alloy│
                    └─────────────────────┘
                              │
                    ┌─────────────────────┐
                    │ Prepare two (2) 20 pound│
                    │ compacts for each size│
                    │   fraction/alloy    │
                    └─────────────────────┘
                              │
                    ┌─────────────────────┐
                    │  HIP all compacts   │
                    └─────────────────────┘
                              │
          ┌───────────────────┴───────────────────┐
┌─────────────────────┐              ┌─────────────────────────┐
│ 4 HIPed compacts of each│          │ Hot work to 1-1/4" ⌀ bars│
│  size fraction/alloy .  │          │ 4 HIPed compacts of each │
└─────────────────────┘              │ particle size fraction/alloy│
                                     └─────────────────────────┘
          └───────────────────┬───────────────────┘
                    ┌─────────────────────┐
                    │      Anneal,        │
                    │       cut,          │
                    │   rough machine     │
                    │   all specimens     │
                    └─────────────────────┘
                              │
                    ┌─────────────────────┐
                    │     Heat Treat      │
                    └─────────────────────┘
                              │
                    ┌─────────────────────┐
                    │        Test         │
                    └─────────────────────┘
                              │
                    ┌─────────────────────┐
                    │     Micros and      │
                    │     analysis        │
                    └─────────────────────┘
```

Figure 1: Schematic of the Overall Program
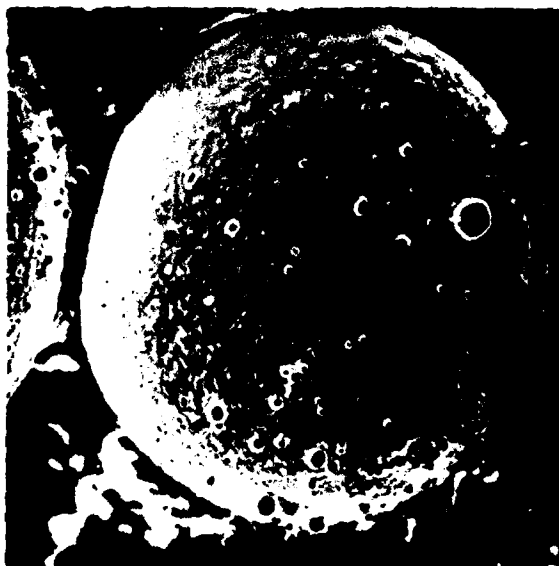
(a)
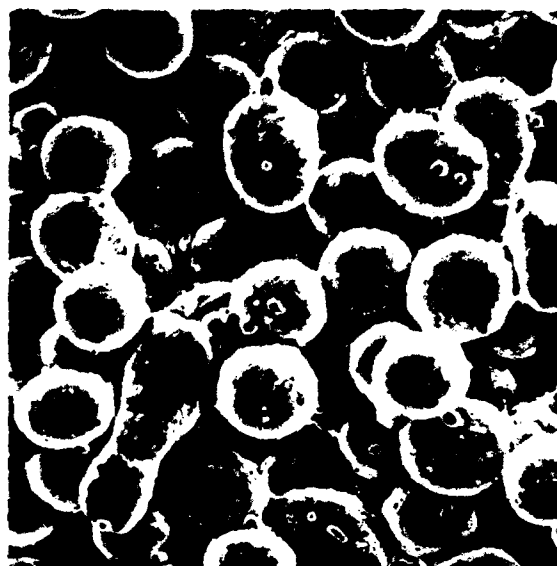
(b)
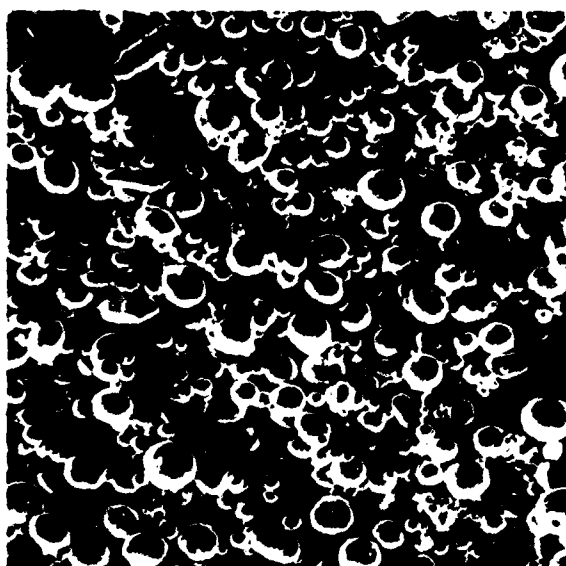
(c)

Figure 2: Micrographs (SEM) of Atomized T15 Powder. (a) ~40 +45,
(b) -200 +230; (c) -400. All magnifications X200.

(a)
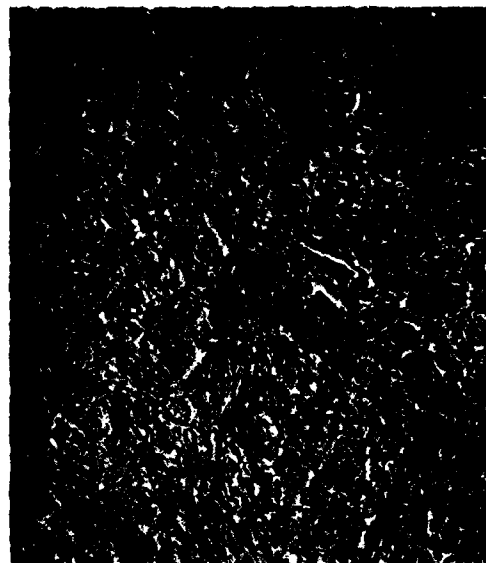
(b)

(c)

Figure 3: Micrographs (TEM/Replicas) of Atomized T15 Powder. (a) -10 +20, X2750; (b) -200 +230, X2750; (c) -400, X7000. All etched with Kalling's Reagent.
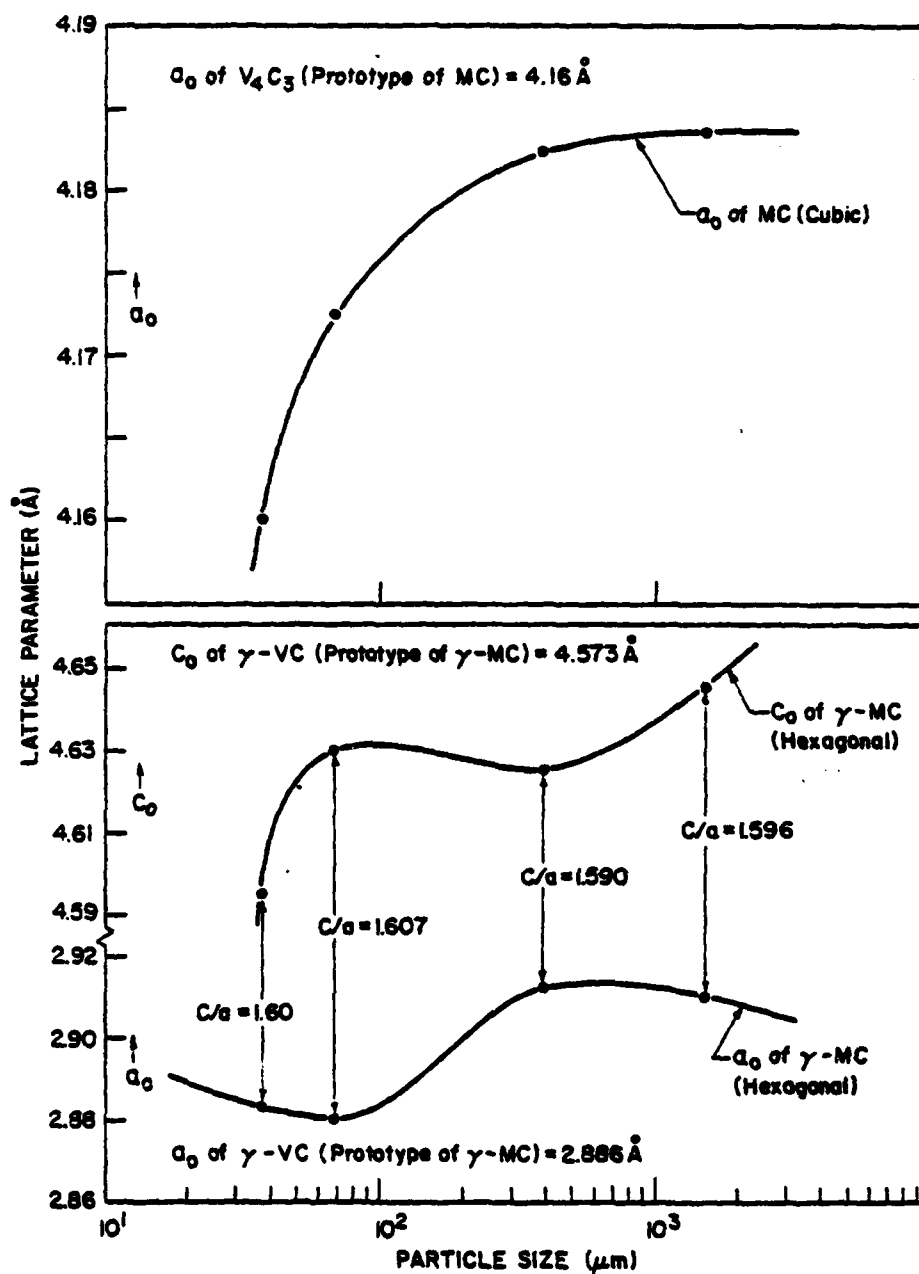
Figure 4: Lattice Parameters of Carbides as a Function of Mean Particle Size - Atomized T15 Powder.
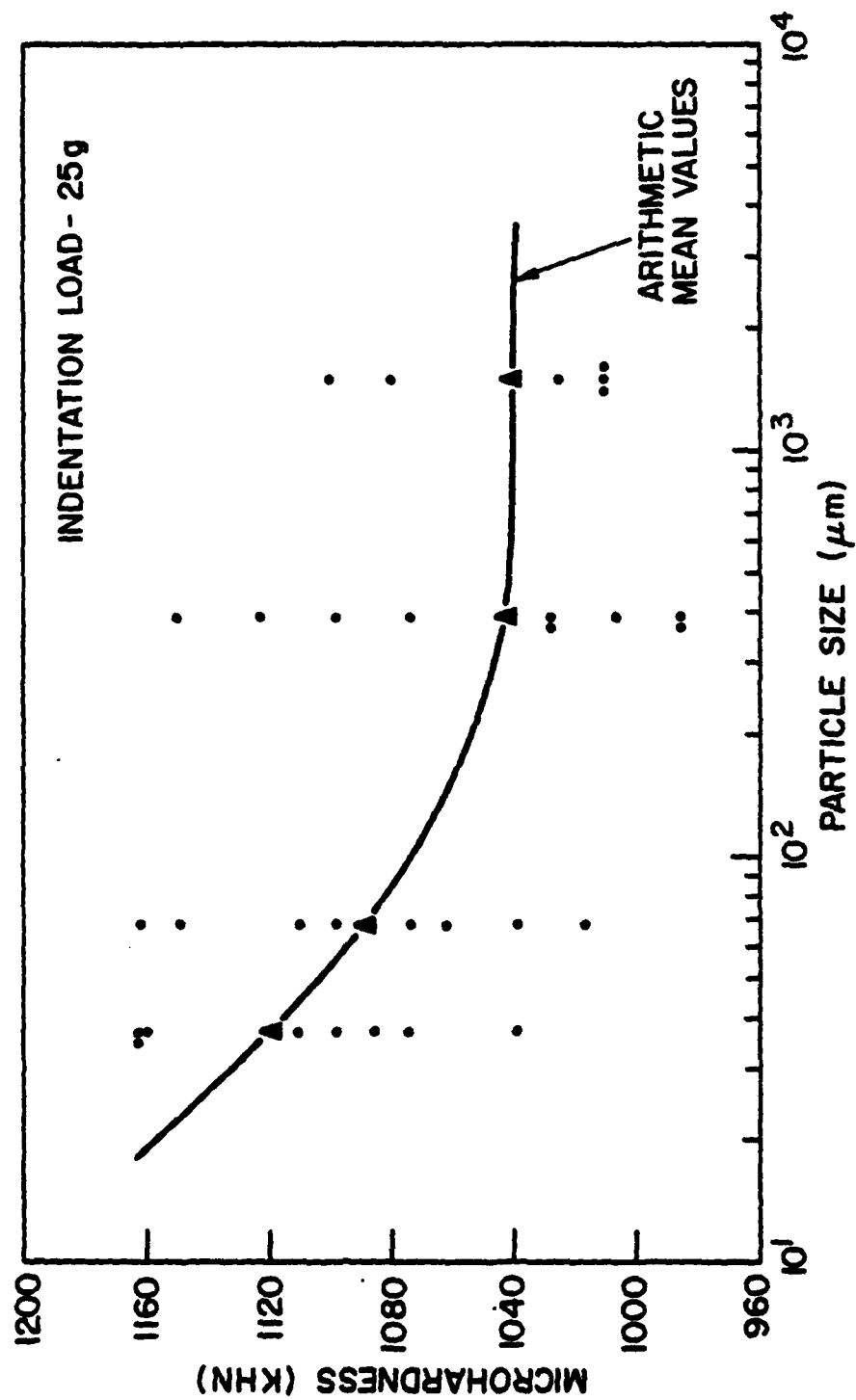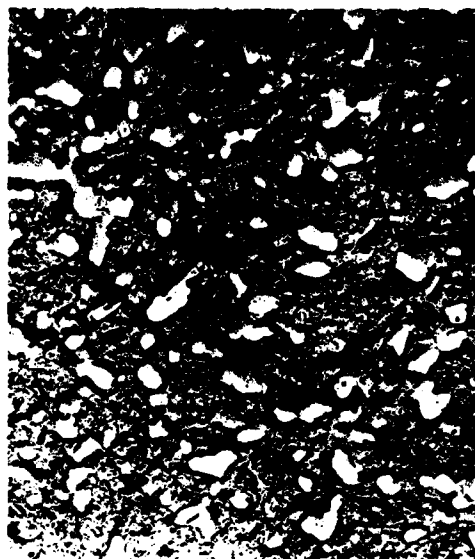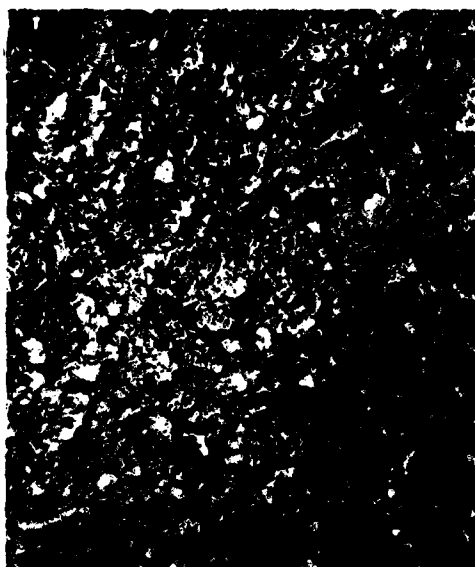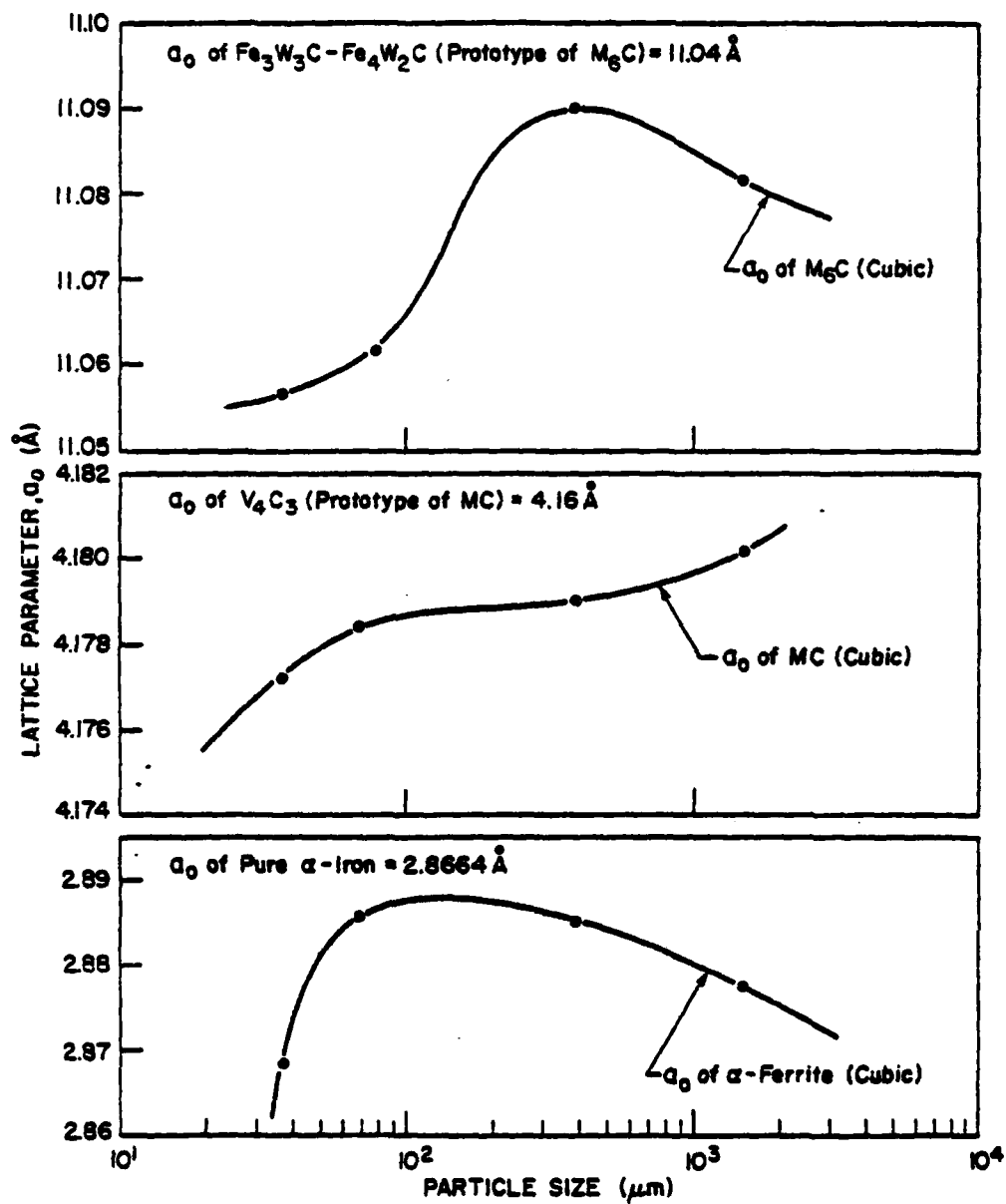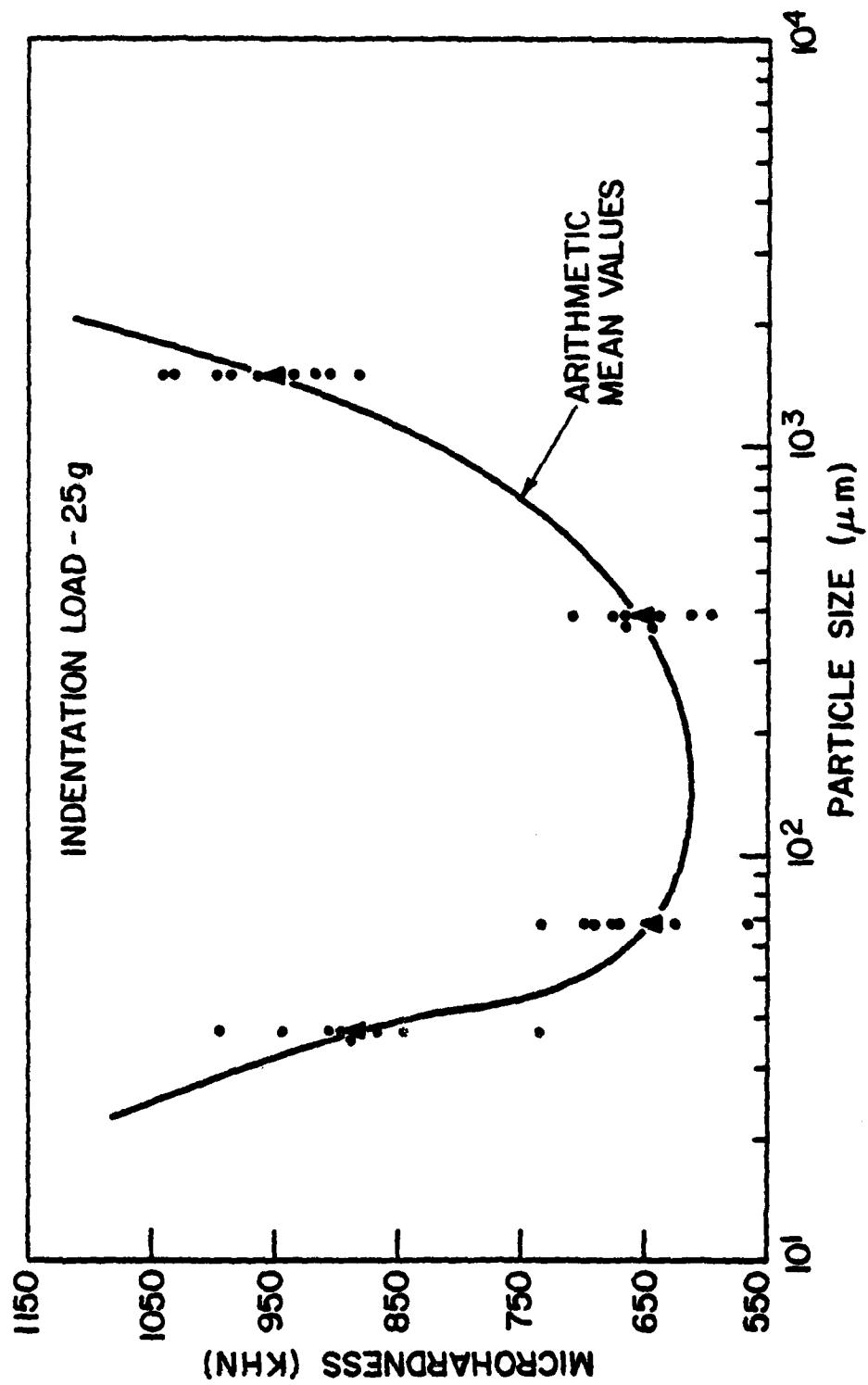
Figure 5: Microhardness of Atomized T15 Powder as a Function of Mean Particle Size.

(a)

(b)

Figure 6: Micrographs (TEM/Replicas) of T15 Annealed Powder. (a) -10 +20, X2750; (b) -400, X2750. Both Etched with Kalling's Reagent.

Figure 7: Lattice Parameters of Matrix and Carbides as a Function of Mean Particle Size - Annealed T15 Powder.

Figure 8: Microhardness of Annealed T15 Powder as a Function of Mean Particle Size.
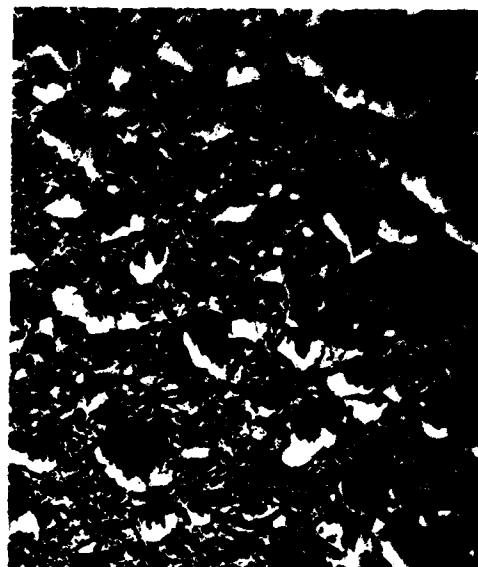
(a)   (b)

Figure 9. Micrographs (TEM/Replicas) of HIPed T15 Materials. (a) -20 +60
           (H1), X2750; (b) -20 +60 (H2), X2750. Both Etched with Kalling's
           Reagent.
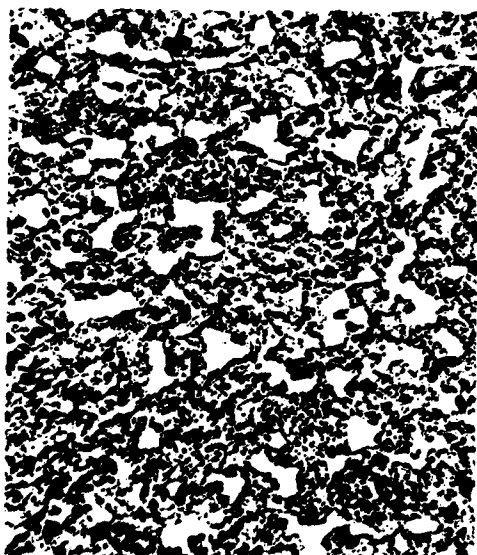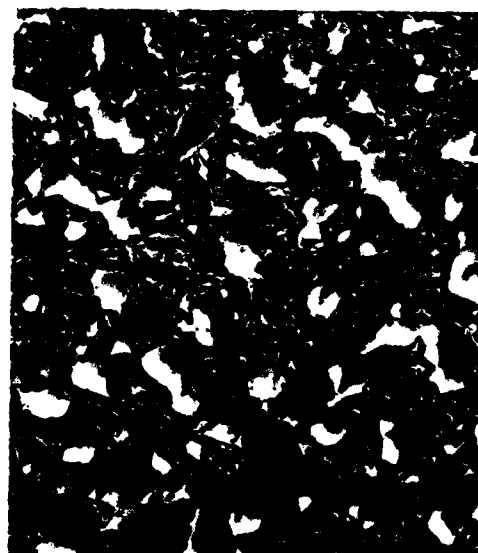
(a)   (b)

Figure 10: Micrographs (TEM/Replicas) of HIPed T15 Material. (a) -325 (H1),
            X2750; (b) -325 (H2), X2750. Both Etched in Kalling's Reagent.
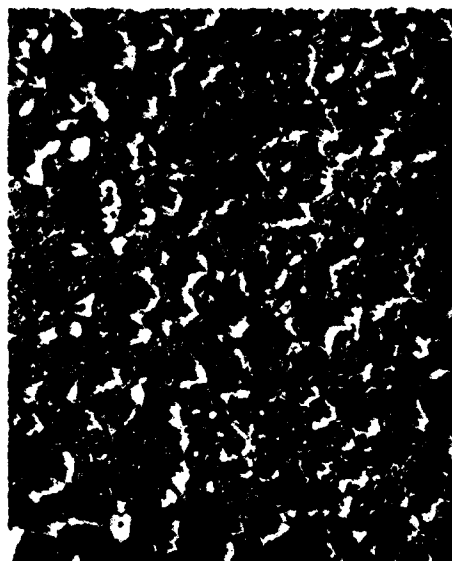
(a)

(b)

Figure 11: Micrographs (TEM/Replicas)of HIPed T15 Material. (a) -20 (H1),
        X2750; (b) -20(H2), X2750. Both Etched in Kalling's Reagent.
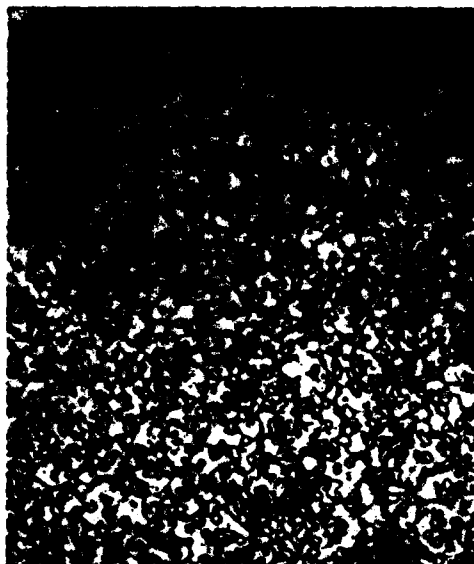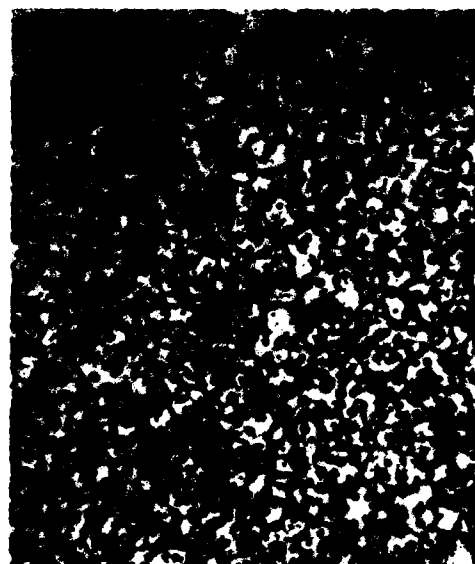
(a)   (b)

Figure 12:   Optical Micrographs of HIPed Plus Heat-Treated Material.
             (a) -325 (H1 + A1); (b) -325 (H1 + A2); Both Etched in 10%
   Nital. Both Magnifications X1000.

(a)   (b)

Figure 13:   Optical Micrographs of HIPed Plus Heat-Treated Material.
             (a) -20 +60 (H1 + A1); (b) -20 +60 (H1 + A2). Both Etched
             in 10% Nital. Both Magnifications X1000.
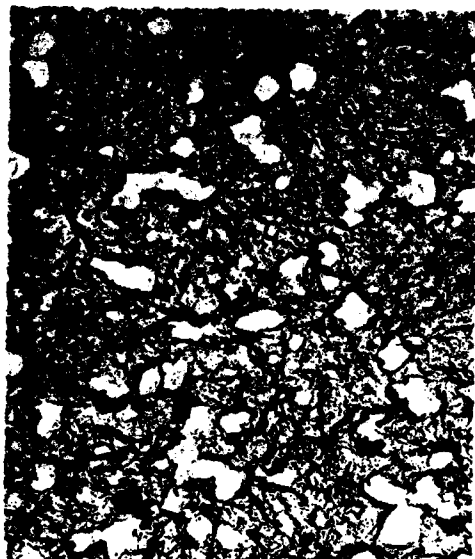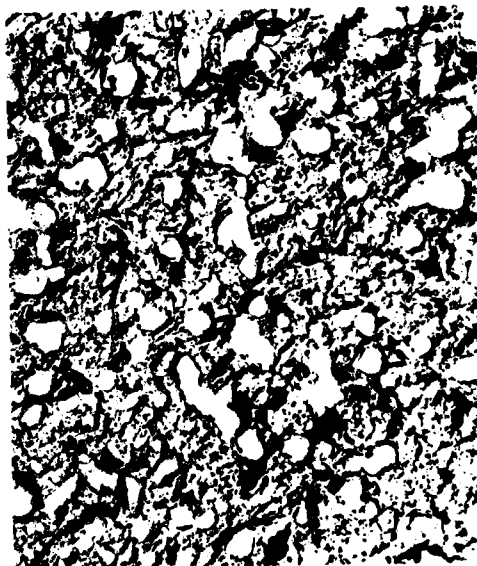
(a)
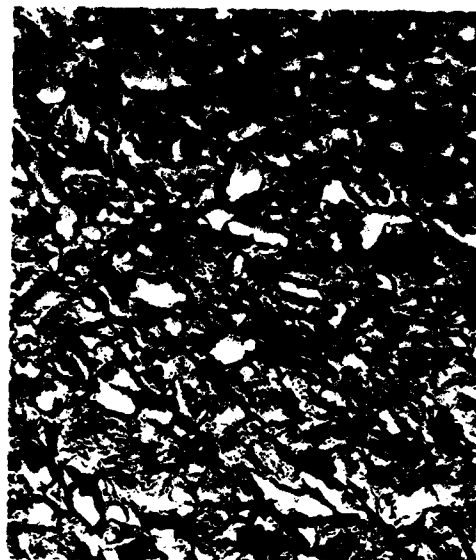
(b)
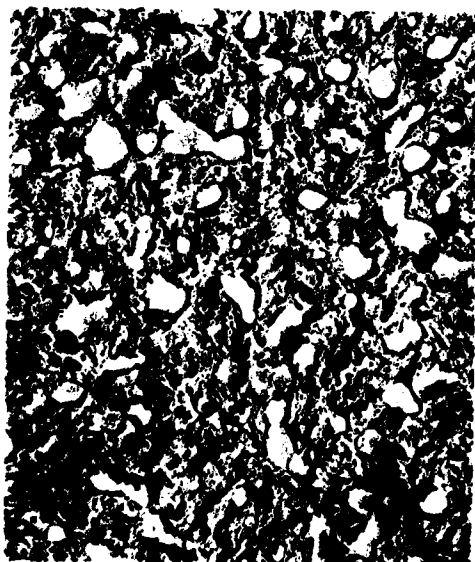
(c)

(d)

Figure 14: Micrographs (TEM/Replicas) of HIPed Plus Heat-Treated Material
From -20 +60 Screen; (a) H1 + A1; (b) H1 + A1 + T1; (c) H1 +
A1 + T2; (d) H1 + A1 + T3. All Etched with Kalling's Reagent.
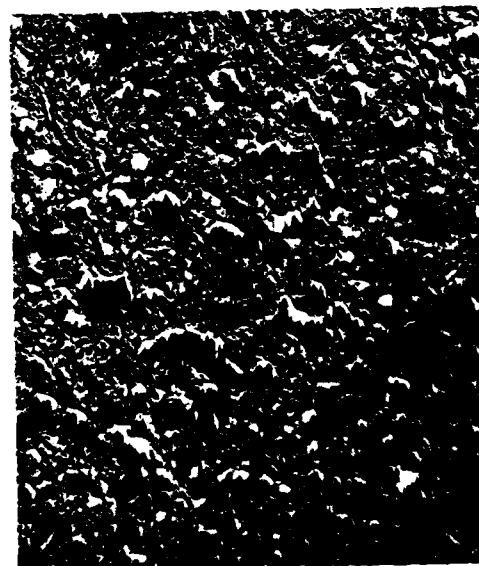All Magnifications X2750.

-45-
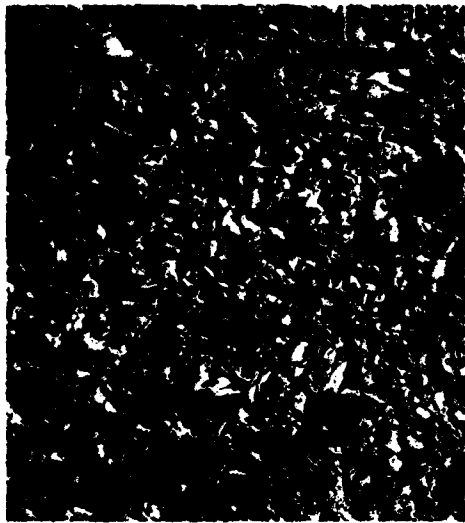
Figure 15: Micrographs (TEM/Replicas) of HIPed Plus Heat-Treated Material From -20 +60 Screen; (a) H1 + A2; (b) H1 + A2 + T1; (c) H1 + A2 + T2; (d) H1 + A2 + T3. All Etched with Kalling's Reagent. All Magnifications X2750.
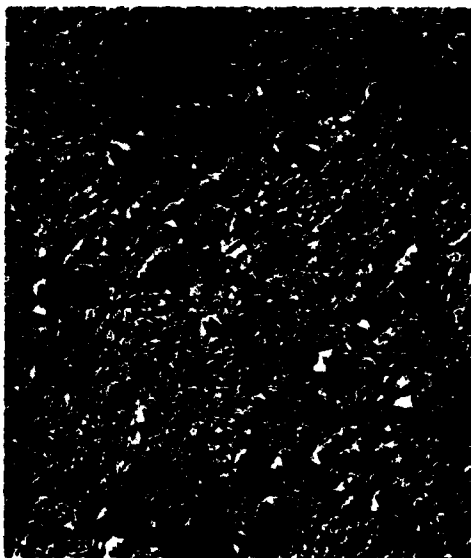
(a)

(b)

(c)

(d)

Figure 16: Micrographs (TEM/Replicas) of HIPed Plus Heat-Treated Material
From -325 Screen;   (a) H1 + A1; (b) H1 + A1 + T1; (c) H1 + A1 + T2;
(d) H1 + A1 + T3. All Etched with Kalling's Reagent. All
Magnifications X2750.

(a)

(b)

(c)

(d)

Figure 17: Micrographs (TEM/Replicas) of HIPed Plus Heat-Treated Material From -325 Screen; (a) H1 + A2; (b) H1 + A2 + T1; (c) H1 + A2 + T2; (d) H1 + A2 + T3. All Etched in Kalling's Reagent. All Magnifications X2750.
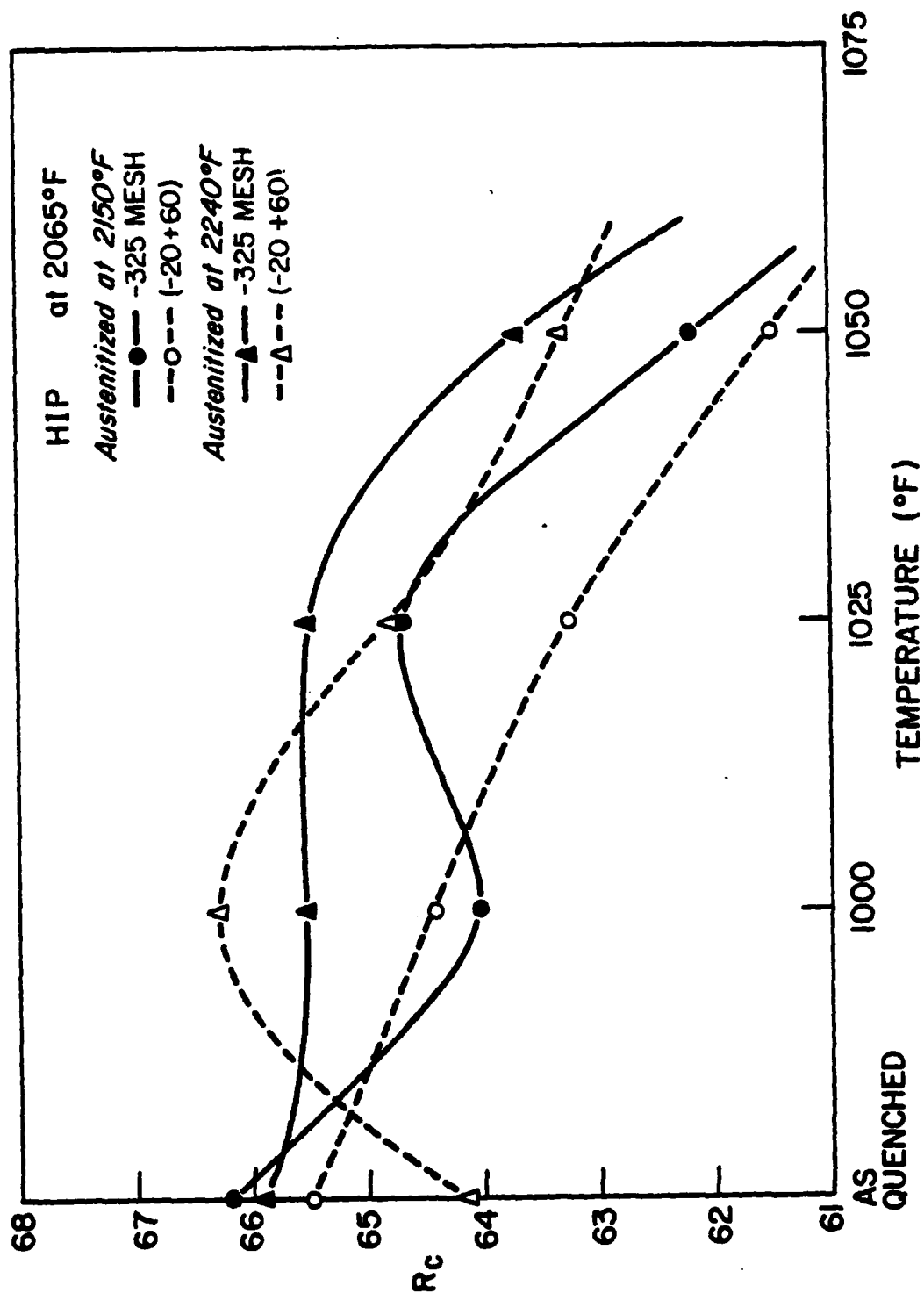
Figure 18: Hardness of HIPed Material as a Function of Screen Size, Austenitizing Temperature and and Tempering Temperature.